Pulse shape discriminators

Z. Seres

KFKI Research Institute for Particle and Nuclear Physics, Konkoly-Thege út 29-33, P.O. Box 49, H-1525 Budapest 114, Hungary

P.D. Zecher* and A. Galonsky

National Superconducting Cyclotron Laboratory and Department of Physics and Astronomy, Michigan State University, East Lansing Michigan, 48824

K. Ieki and Y. Iwata

Department of Physics, Rikkyo University, 3 Nishi-Ikebukuro, Toshima, Tokyo 171-8501, Japan

D.E. Carter

Edwards Accelerator Laboratory, Department of Physics and Astronomy, Ohio University, Athens, Ohio 45701

(April 4, 2003)

Abstract

We summarize and systematize the pulse shape discrimination methods published in the last ten years for n/γ discrimination.

I. INTRODUCTION

In some liquid scintillators as e.g. the NE 213 the quenching, the thermal deexcitation of the fast light component depends strongly on the specific ion-

*Crrent address: Investor Analytics LLC, 80 Broad Street, New York, NY 10004

ization of the charged particles [1]. Analyzing the shape, the time structure of the light pulse one can separate the energetic proton induced scintillation from that of the electrons or μ-mesons. This difference makes possible the identification of neutral particles like neutron and γ-ray events too. The building of a neutron-wall detector put forward the problem of the pulse shape discrimination in the NSCL.

II. RECENT PSD METHODS

The third generation charge integrating ADC-s make possible to measure and analyse the PMT signal directly from the anode. Using 50 Ω load resistor the anode signal can be connected directly or through a terminated ohmic splitter to the 50 Ω input of the ADC.

The light pulse of the NE 213 liquid scintillator has two main components as shown in fig. 1 measured by the one photon method [2]. The method is described in Appendix I. The decay time of the fast component is about 3.2 ns while the slow component about 100 ns. The ratio of the slow component to the total light is approximately 28 and 13% for the neutrons and γ-rays, respectively.

The particle can be identified compairing the head charge (fast component) or the tail charge (slow component) to the total charge. The analysis of the pulse shape, the separation of the light components can be performed by cutting in time or after shaping the pulse cutting in charge.

The simplest method is cutting in time. The anode signal is splitted by a three way terminated ohmic splitter. From one signal a cca. 300 ns gate is formed which opens the ADC linear gate and the other two signals are put onto the ADC inputs delayed so that the tail charge signal preceeds the gate by a well defined time in the range of 25–35 ns, and the total charge signal

sits in the gate fully with a delay of 10–20 ns (in case of LeCroy 4300 FERA more than 30 ns) shown in fig. 2 [3]. The advantage of the method is that it uses commercial charge sensitive ADC and gate and delay generator. The signals must be strictly correlated to the gate. Therefore the synchronous gate PSD method (SG PSD) can be applied only for one or for limited number of detectors or PMT-s and in case of multiple detector usage it requests a lot of additional units (gate and delay generators and linear gates or ADC with separate gates).

For shaping the pulses two modes were used for PSD circuits. The fast component can be selected by differentiating the pulse or cutting with a clipping cable as shown in fig. 3. In both cases a bipolar signal is produced the negative charge is measured and the positive part must be cut. The method differentiating the pulse was used by J. Tőke et al. [4]. The dynode pulse was differentiated and the leading short positive charge was cut by a biased amplifier and the negative overshoot was integrated measuring the fast component. At the neutron-wall of the NSCL the anode pulse was shortened by a reflecting short closed clipping cable (CC PSD method) and the positive charge was cut by the input linear gate of the commercial ADC.

III. CABLE CLIPPING PSD

In the NSCL a new large area position sensitive neutron detector, the neutron wall detector was built with possible small scattering material compared to the sensitive volume [5]. The neutron wall was planned basically for experiments with radioactive beams. The two walls consist of 25 pieces of $6 \times 6 \times 200$ cm^3 glass tubes each filled with NE 213 liquid scintillator. Because of the large volume of the scintillator the neutron wall has relatively large cosmics background (cca. 350 counts/s per cell) and even if there were no

γ radiation the individual identification of the particles has vital importance. The synchronous gate method could be used hardly already for one cell of the neutron wall. The uncertainty of the PMT timing is in the range of ± 12 ns due to the position dependence of the detection which makes impossible to apply common ADC gate for the left and right PMT-s. Further in certain nuclear physics experiments measuring two neutron events one must let to be measured any pair of the cells simultainously. Therefore we had to work on a new kind of PSD method [6]. We have recognized that the input linear gate of the LeCroy 2249W charge sensitive ADC cuts the positive charge at a rather low level which can be used for PSD with charge shaping method. We applied a clipping cable for shortening the pulses. The reflected positive charge from a short cut cable will compensate the tail charge producing a bipolar pulse. The leading negative pulse represents the fast component and the positive part of the bipolar signal will be cut by the linear gate of the ADC input.

In fig. 4 there are plotted the relative integrated spectra of the light pulses for neutrons and γ-rays calculated from the fitted functions in fig. 1. The difference of the two lights is maximum about 16 ns so the length of the clipping cable was chosen to 8 ns where the fast components are about 93 and 87% of the total light for γ-rays and neutrons.

(In the Appendix II. we summarize the history of the CC-PSD method for internal usage and it need not be part of the publication.)

The clipping cable must be actively separated from the source therefore an emitter follower was implemented between the clipping cable and the source shown in fig. 5. In the figure there are shown two channels one for the non attenuated and one for the 12 dB attenuated anode signal by a terminated 2-way splitter at the input. The advantage of the pulse shaping method is that the component charge can be measured asynchronous with a common

gate in case of several PMT-s too.

The advantage of the emitter follower is that it separates the cable and the fast signal from the input by a large input impedance which makes not necessary to divide the anode signal by an ohmic splitter for Q_{tot} and Q_{fast}. The CC PSD compares the fast component to the total charge therefore the separation line in the Q_{fast} vs Q_{tot} scatter plot is rather linear even if the PMT is nonlinear.

The output of the emitter follower has a low impedance ($< 50\ \Omega$) therefore the cable reflected signal will be rereflected from the emitter producing a damped oscillation. The oscillating part remains positive making 4–5 oscillations with an amplitude about 20% of the leading negative pulse and lasts no longer than 100 ns. The oscillation can be avoided terminating the emitter but its price is an attenuation of the signals by a factor of 2.2. The gate is started by the first PMT fireing and must cover the integration time (300 ns) plus the dynamic range of the neutron time of flight, i.e. must wait for the arrival of the smallest energy neutron to be measured.

Below we compare the performaces of the CC PSd and the SG PSD methods in similar conditions used in the n-wall detector. The anode signal was delayed by 100 ns cable delay for the analogue signals and the logical signals were produced from the 12^{th} dynode of the PMT XP4312B inverted by a pulse transformer (MCL T1-6T). For the study of the different methods we used a 120 ml NE 213 commercial scintillator on an XP2020 PMT with anode and 14^{th} dynode signals with a 2 way splitter for the SG PSD and a unit of the n-wall for the CC PSD using LeCroy 2249W ADC.

The separation is based on the comparision of the Q_{fast} or Q_{slow} component and the Q_{tot}. The PSD can be demonstrated in the Q_{fast} (or Q_{slow}) vs Q_{tot} scatter plot. In fig. 6 there are shown the PSD scatter plots of the CC PSD and the SG PSD methods. For the comparions of the methods one can

calculate a figure of merit (FOM) from the PSD plots. At certain Q_{tot} bins the Q_{fast} or Q_{slow} spectra can be fitted by two Gaussian distributions and taken the

$$FOM = \frac{P_\gamma - P_n}{2\sqrt{2\ln 2}(\sigma_\gamma + \sigma_n)},$$

where P is the peak position and σ is the standard deviation of γ particle and neutron peaks. The figure of merits differ less than 5% for the CC PSD and SG PSD methods as shown in fig. 7.

IV. PULSE SHAPING BY DIFFERENTIATION

We tested the PSD quality using the differentiation of the scintillation pulse too. The clipping cable was removed and the coupling condensator 4.7 nF was replaced by 470 pF capacitance (RC=28 ns). The PSD plot is shown in fig. 8 and the FOM is compared to the CC PSD and SG PSD methods in fig. 7. The FOM of the PSD with differentiation is somewhat less but not more than 5% of the CC PSD. We checked the differentiation direct from a passive splitter too. It is effective but the emitter follower saves the division of the termination.

V. ROLE OF THE ADC INPUT LINEAR GATE

In the CC PSD applied for the NSCL n-wall the ADC input must cut the positive charge therefore the threshold depends on the specific ADC type. For the comparision of some charge sensitive ADC-s in fig. 9 there are plotted the lower section of the Q_{fast} vs Q_{tot} scatter plots of Pu-Be neutron source measured at one end of a cell of the n-wall. The Q_{tot} is calibrated: 113 channels corresponds to 1 MeVee and the Q_{fast} is measured by three different charge sensitive ADC-s.

With LeCroy 2249W ADC the threshold is less than 0.5 MeVee, with the Phillips 7167 ADC about 1.2 MeVee, while with the LeCroy 4300 FERA about 6.5 MeVee in the neutron-wall application. The slope of the PSD plots is the same only the threshold of the fast component changes shifting higher the energy cut. The cut is rather sharp. For the part of the signals less than the cut level of the positive charge the negative charge will be fully compensated and the part overcoming the cut level, the top of the positive charge will be cut resulting in a net negative charge. The choice of the ADC must be a compromise between the energy threshold and the speed of data taking. The LeCroy ADC 2249W is rather slow its conversion time is 84 μs, while 7.2 μs for the Phillips 7167. The effect of the termination of the emitter follower is also shown in fig. 9. The fast component is reduced by a factor 2.2 resulting in a less slope and higher energy threshold about 1.5 MeVee.

VI. EPILOG

We must confess that although the above argumentations are true they must be reconsidered in the results got with the differentiation method. We were enthusiastic working on the CC PSD and it was operating very successfully although we didn't analyse how does it function. From the summary of the PSD methods published here it turned out that the basic recognition was that the charge sensitive ADC LeCroy 2249W cuts the positive charge of a reshaped bipolar signal on a fairly low level. The shaping of the pulse by clipping cable is as good as the differentiation. For the cable forming one must implement an emitter follower but the differentiation of the signal can be used with a passive splitter and perhaps even with a simple Lemo T connector.

The other point is the important role of the ADC input circuit. If the LeCroy 2249W ADC is unacceptable slow one must look for an other ADC

or one has to furnish the PSD circuit with a discriminating element like in ref. 4.

Acknowledgements. We are grateful for the support of the National Science Foundation under Grant Nos. PHY 95-28844 and to OTKA T032113 of the Hungarian Science Foundation.

VII. APPENDIX I

The decay time of the scintillations can be measured by the one-photon method [2]. The scintillator is coupled to a PMT and an other PMT is placed far enough to detect from a flash only one photon or less (fig. 10). The solid angle can be set by the distance and with a diaphragm. For orientation we can use that 1 MeV energy deposited in the NE123 liquid scintillator means about 10^4 photoelectrons. The PMT2 must be discriminated at the one photon level. It will sample the photons measuring the probability distribution of the photon emission from the excited states. The setup used for the one photon measurement is shown in fig. 11.

The time spectrum of the photon distribution is analysed searching two main components sitting on a constant background. The analytic function of the components are searched as the convolution of a Gaussian excitation and an exponential decay. The convolution can be calculated numerical using the polynomial and rational approximation of the error function [7]. The neutron and γ-ray pulses are identified and separated with the SG PSD.

The light pulse is the convolution of Gaussian excitation and an exponential decay. In the interaction in the t_0 time there is produced N excited molecule with a standard deviation of σ. The excited molecules will decay with a τ decay time emitting a scintillation light quantum.

$$L(t) = \int_{-\infty}^{t} \frac{N}{\sqrt{2\pi}\sigma} \exp\left(-\frac{(t'-t_0)^2}{2\sigma^2}\right) \frac{1}{\tau} \exp\left(-\frac{t-t'}{\tau}\right) dt'.$$

Introducing the $p = t - t'$ new variable $p_0 = t - t_0$ and

$$L(p) = \frac{N}{\sqrt{2\pi}\sigma\tau} \int_0^\infty \exp\left(-\left(\frac{(p-p_0)^2}{2\sigma^2} + \frac{p}{\tau}\right)\right) dp.$$

The exponential

$$\frac{1}{2}\left(\left(\frac{p-p_0}{\sigma} + \frac{\sigma}{\tau}\right)^2 + \frac{2p_0}{\tau} - \frac{\sigma^2}{\tau^2}\right)$$

the integrandus is a new Gaussian distribution of unity standard deviation,

$$L(p_0) = \frac{N}{\sigma\tau} \exp\left(\frac{\sigma^2}{2\tau^2} - \frac{p_0}{\tau}\right) \frac{1}{\sqrt{2\pi}} \int_0^\infty \exp\left(-\frac{\left(\frac{p-p_0}{\sigma} + \frac{\sigma}{\tau}\right)^2}{2}\right) dp,$$

which integral is numerically known, the error function:

$$L(p_0) = \frac{N}{\sigma\tau} \exp\left(\frac{\sigma^2}{2\tau^2} - \frac{p_0}{\tau}\right) \left[\sigma \operatorname{erf}\left(\frac{p-p_0}{\sigma} + \frac{\sigma}{\tau}\right)\right]_0^\infty$$

$$L(p_0) = \frac{N}{\tau} \exp\left(\frac{\sigma^2}{2\tau^2} - \frac{p_0}{\tau}\right) \left(1 - \operatorname{erf}\left(\frac{\sigma}{\tau} - \frac{p_0}{\sigma}\right)\right)$$

$$L(t) = \frac{N}{\tau} \exp\left(\frac{\sigma^2}{2\tau^2} - \frac{t-t_0}{\tau}\right) \left(1 - \operatorname{erf}\left(\frac{\sigma}{\tau} - \frac{t-t_0}{\sigma}\right)\right).$$

The error fuction approximated by the rational polynom [7]:

$$\operatorname{erf}(x) = 1 - \frac{1}{\sqrt{2\pi}} \exp\left(-\frac{x^2}{2}\right)(a_1 t + a_2 t^2 + a_3 t^3) + \epsilon(x),$$

where $t = \frac{1}{1+px}$, $p = 0.33267$, $a_1 = 0.4361836$, $a_2 = -0.1201676$ és $a_3 = 9372980$. The error of the approximation $|\epsilon(x)| < 1 \cdot 10^{-5}$.

VIII. APPENDIX II

P. Zecher on the advice of D. E. Carter applied a short closed cable to an ohmic splitter and found a slight pulse shape discrimination for neutrons and γ-rays. He had a good luck for he used a 3-way splitter and a LeCroy 2249W charge sensitive ADC. The LeCroy 2249W ADC does the favour cutting the positive charge on a rather low level. Phil's results were promising but the pulse shaping using a passive splitter with a clipping cable is not a correct solution by two reasons *i*) the cable makes wrong the termination which can

produce reflections and *ii*) the reflected signal will be superimposed on all the branches of the splitter reducing the differences of the Q_{tot} signals of neutrons and γ-rays.

We investigated the passive splitters furnished with a 8 ns clipping cable. The simplified schemes are shown of a 2-way and 3-way splitter in fig. 12 neglecting the stray capacitances. The fast components contain 50% reflected signal while the total charges about 20% and 13% for the 2-way and 3-way splitters, respectively. The contribution of the reflected signal is less if the splitting is larger. We tested the PSD with a 2-way and a 3-way splitter. In fig. 13 the Q_{fast} vs Q_{tot} PSD scatter plot is shown for the 2-way splitter with a 8 ns clipping cable. The reflected signal almost perfectly compensates the slow component in the Q_{tot} giving no PSD splitting of neutron and γ-rays. With the 3-way splitter the PSD plot is splitted a little resulting in some PSD possibility shown in fig. 13. Please compare to fig. 6. The effect of the rescattered positive charge is seen in the reduction of the Q_{tot}. In order to compare the spectra to the calculations let us take the ratio of the slopes Q_{fast}/Q_{tot} of the CC on 2-way and 3-way splitters. The ratio is 0.87 from the measured spectra and from the calculations as well. The figure of merit of the PSD got with a clipping cable on a 3-way splitter is plotted in fig. 7.

The above results show the importance of the active separation of the cable from the source in the CC-PSD method. Therefore we applied an emitter follower for the Q_{fast} branch. The emitter follower has further advantages one can save the 2-way splitter for the Q_{tot} and Q_{fast} signals driven by the same 50 Ω source resulting in a gain of 2.

IX. FIGURE CAPTIONS

Fig. 1. Light pulse shape of NE 213 liquid scintillator for neutrons and γ-rays measured by one photon method with Pu-Be neutron source.

Fig. 2. Principle of synchronous gate PSD method — cutting in time.

Fig. 3. Principle of cable clipping and differentiating PSD.

Fig. 4. Relative integrated light spectra.

Fig. 5. Scheme of the cable clipping pulse shape discrimination (CC PSD) circuits (nonattenuated and attenuated) for one PMT.

Fig. 6. PSD scatter plots of Pu-Be neutron source measured by Q_{slow} vs Q_{tot} for SG PSD and Q_{fast} vs Q_{tot} for CC PSD methods.

Fig. 7. Figure of merit for the SG PSD, CC PSD, and differentiation methods. Additional the cable clipping on a 3-way splitter is also shown.

Fig. 8. PSD scatter plots Q_{fast} vs Q_{tot} for CC and differentiaton PSD.

Fig. 9. The comparision of the PSD plots the fast component measured with a.) LeCroy 2249W ADC (11 bit), b.) the same but the emitter follower terminated, c.) with Phillips 7167 ADC (12 bit), and d.) with LeCroy 4300 FERA (qfst measured in the place of qatt total charge).

Fig. 10. Layout of the measurement of the scintillation light pulse shape with the one photon method.

Fig. 11. The setup used for the one photon measurement of the scintillation light pulse. The labels are: 2W two way passive splitter, CFD constant fraction discriminator, G&D gate and delay generator, FD fast discriminator, FAN logical fan in/out, STR status register, and D cable delay.

Fig. 12. The simplified schemes of clipping cables on two- and three-way 50 Ω terminated splitters.

Fig. 13. PSD scatter plots Q_{fst} vs Q_{tot} for clipping cable on 2-way and 3-way passive splitters.

REFERENCES

[1] J.B. Birks, The theory and Practice of Scintillation Counting, Pergamon Press, Oxford, 1964, pp. 219-227 and 392-394.

[2] M. Moszyński, B. Bengston, Nucl. Instr. & Meth. **142** (1977) 417

[3] J. H. Heltsley, L. Brandon, A. Galonsky, L. Heilbronn, B. A. Remington, S. Langer, A. Vander Molen, J. Yurkon, J. Kasagi, Nucl. Instr. & Meth. **A263** (1988) 441

[4] J. Tőke, S.A. Masserant, S.P. Baldwin, B. Lott, W.U. Schroder, and X. Zhao, Nucl. Instr. & Meth. A334 (1993) 653

[5] P.D. Zecher, A. Galonsky, J.J. Kruse, S.J. Gaff, J. Ottarson, J. Wang, F. Deák, Á. Horváth, Á. Kiss, Z. Seres, K. Ieki, Y. Iwata and H.R. Schelin, Nucl. Instr. & Meth. A401, (1997) 329

[6] P.D. Zecher, A. Galonsky, D.E. Carter, and Z. Seres, MSUCL-1256 preprint, February 2003, East Lansing, MI-48824

[7] M. Abramowitz and J. A. Stegun, Handbook of mathematical functions with formulas, graphs, and mathematical tables (National Bureau of Standards, Applied Mathematics Series 55, Washington D.C. 1966) p. 932

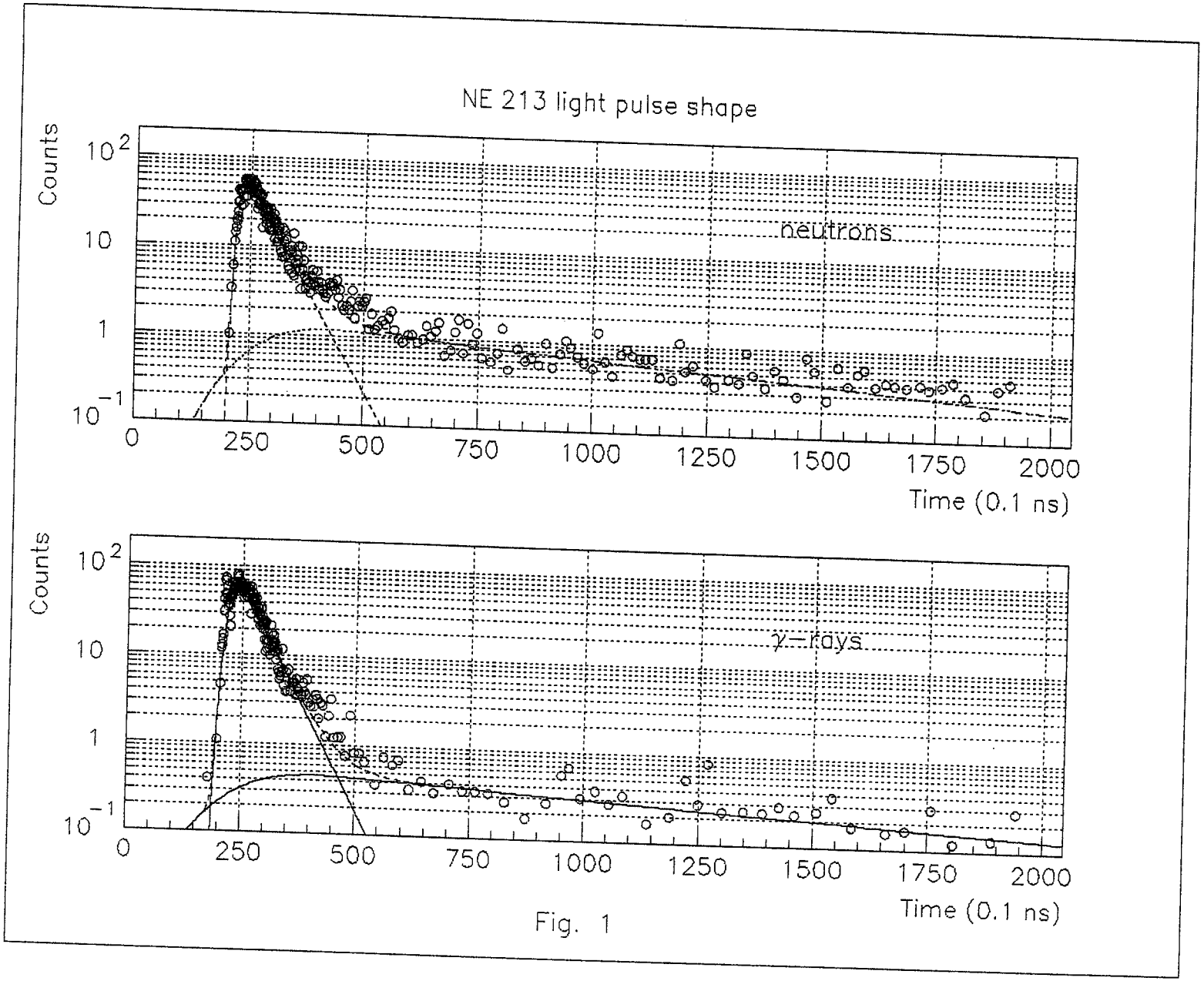
NE 213 light pulse shape
Counts
10^2
10
1
10^{-1}
0
250
500
750
1000
1250
1500
1750
2000
neutrons
Time (0.1 ns)
Counts
10^2
10
1
10^{-1}
0
250
500
750
1000
1250
1500
1750
2000
γ-rays
Time (0.1 ns)

Fig. 1

Synchronous gate PSD

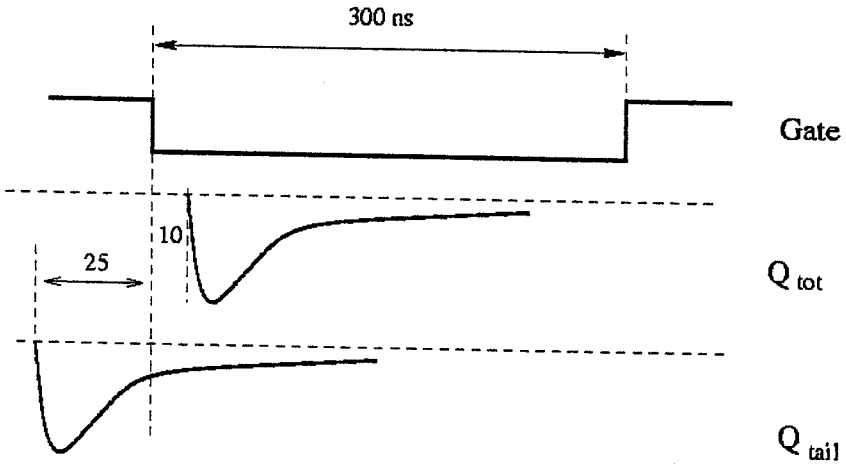

Fig. 2

Pulse shaping for asynchronous PSD

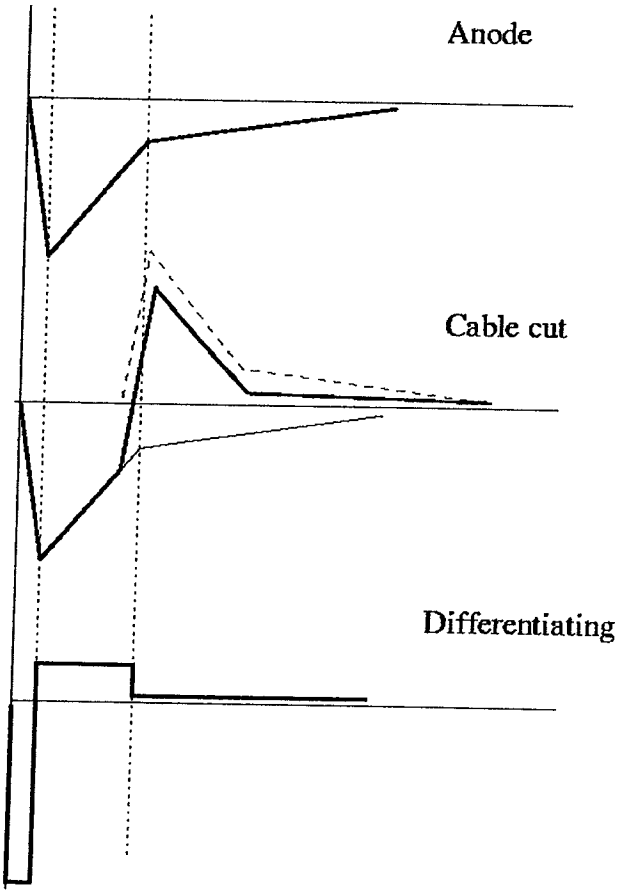

Fig. 3

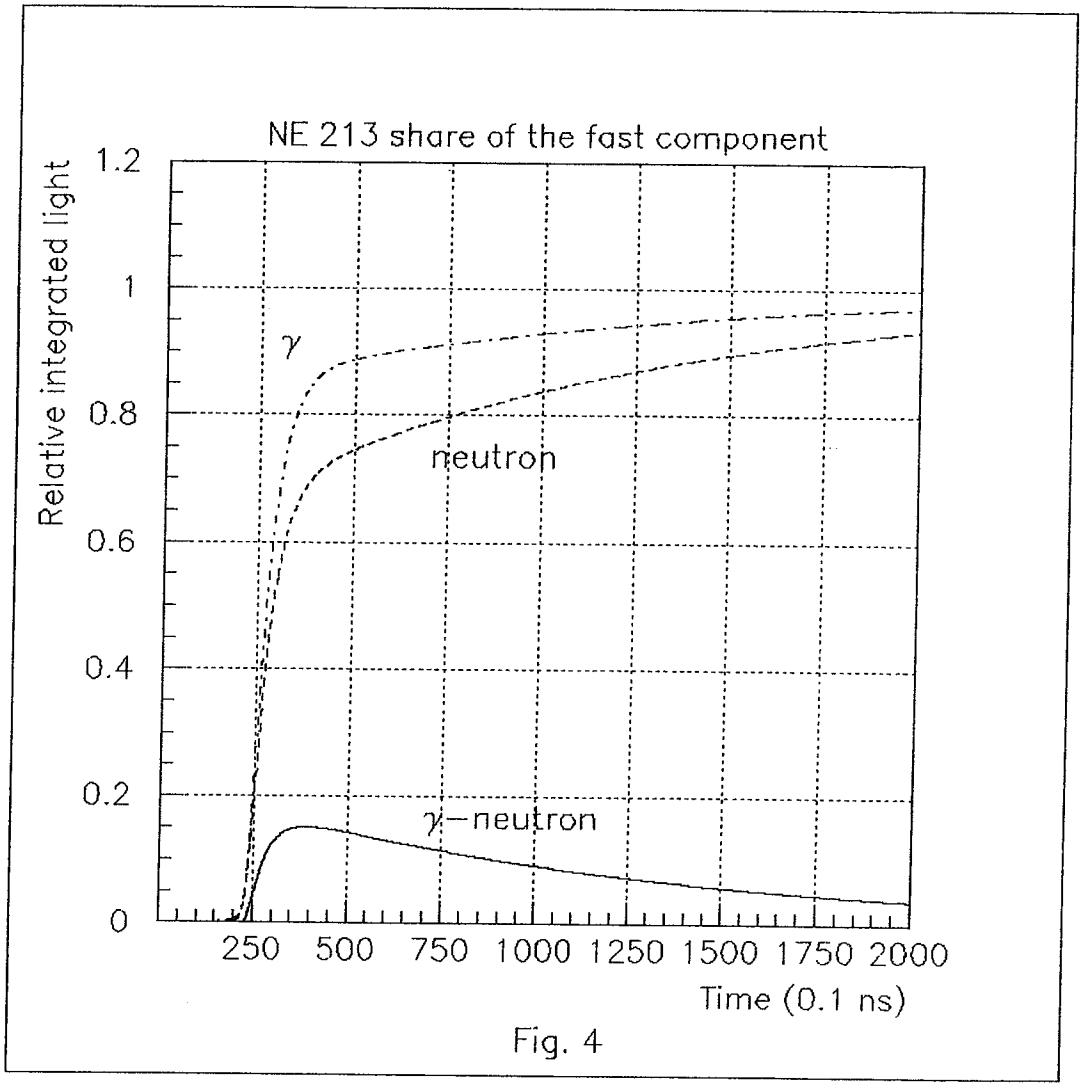
NE 213 share of the fast component
Relative integrated light
1.2
1
0.8
0.6
0.4
0.2
0
γ
neutron
γ−neutron
250
500
750
1000
1250
1500
1750
2000
Time (0.1 ns)

Fig. 4

Pulse shaping of CC–PSD for neutron wall

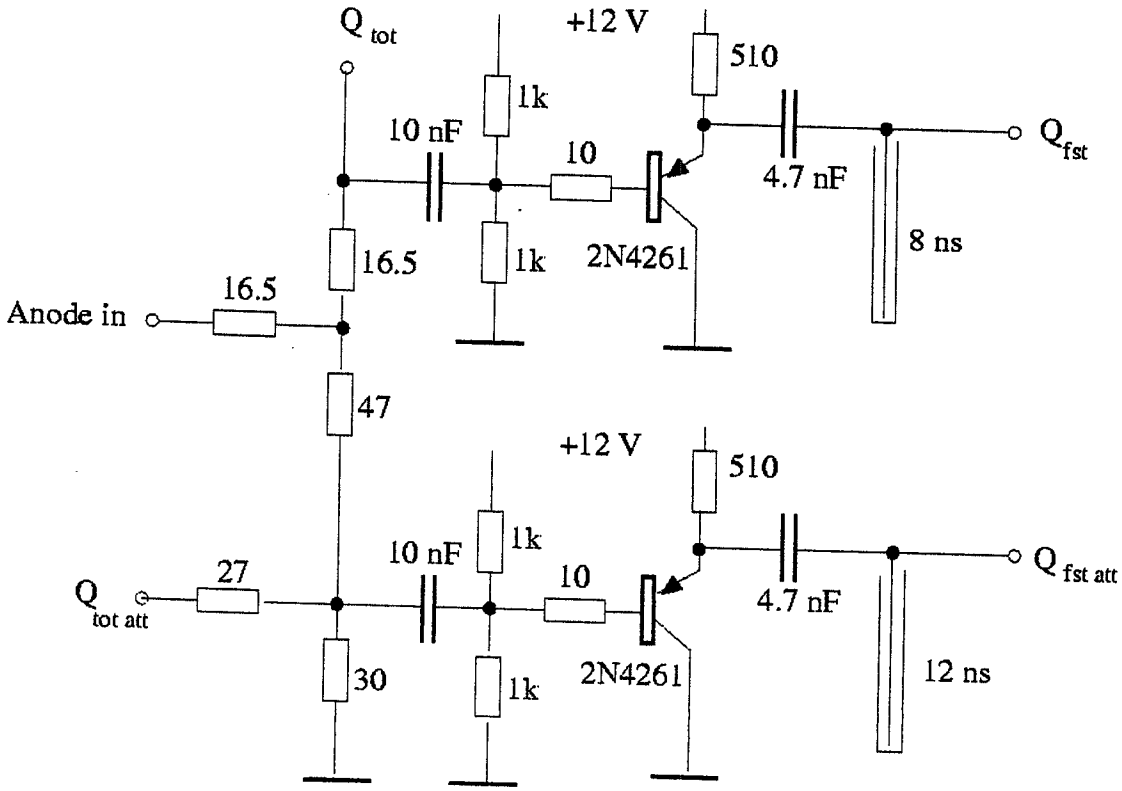

Fig. 5

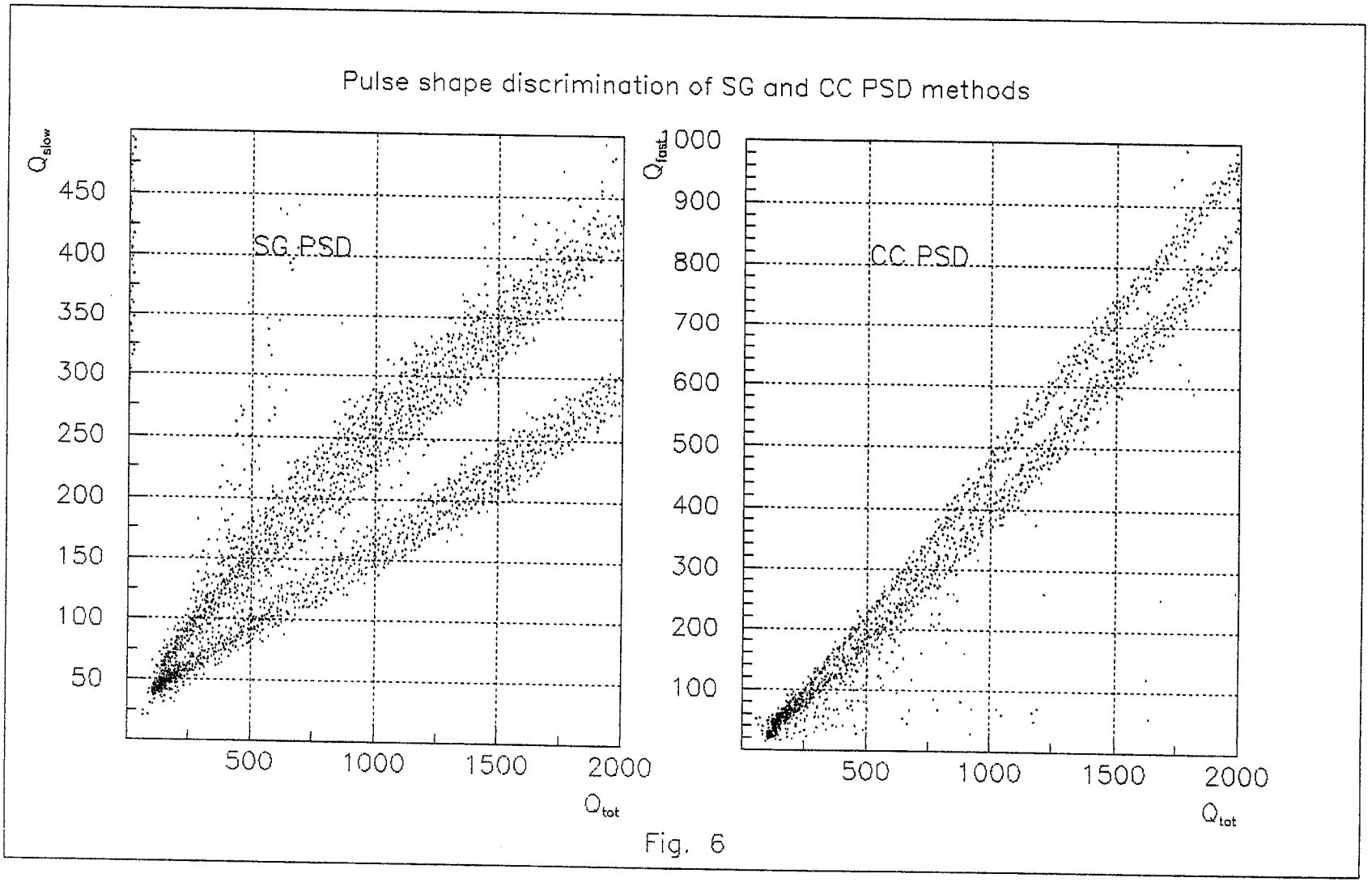
Pulse shape discrimination of SG and CC PSD methods
SG PSD
CC PSD
Q_{slow}
Q_{fast}
Q_{tot}
Q_{tot}
50
100
150
200
250
300
350
400
450
100
200
300
400
500
600
700
800
900
1000
500
1000
1500
2000
500
1000
1500
2000

Fig. 6

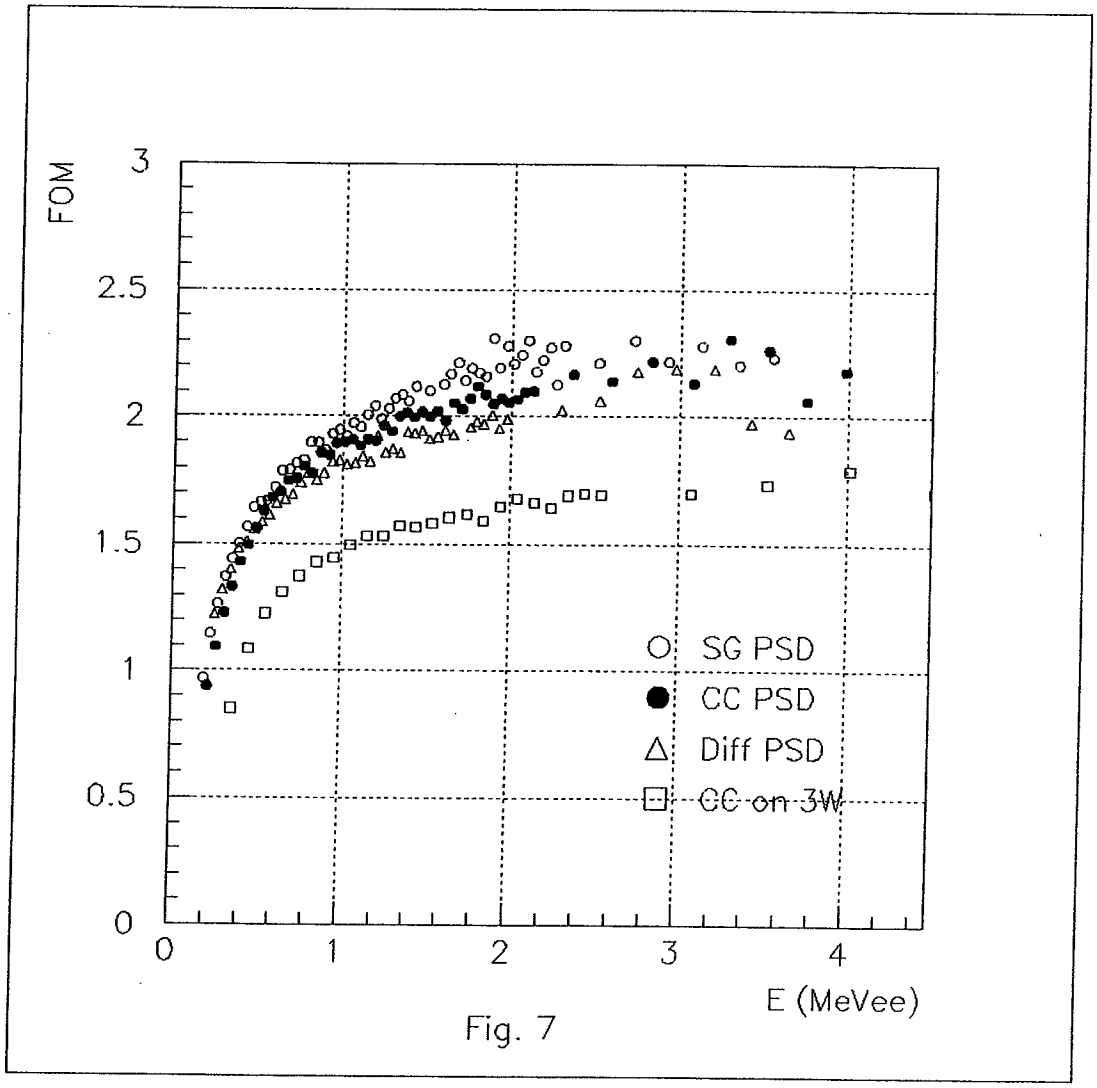

Fig. 7

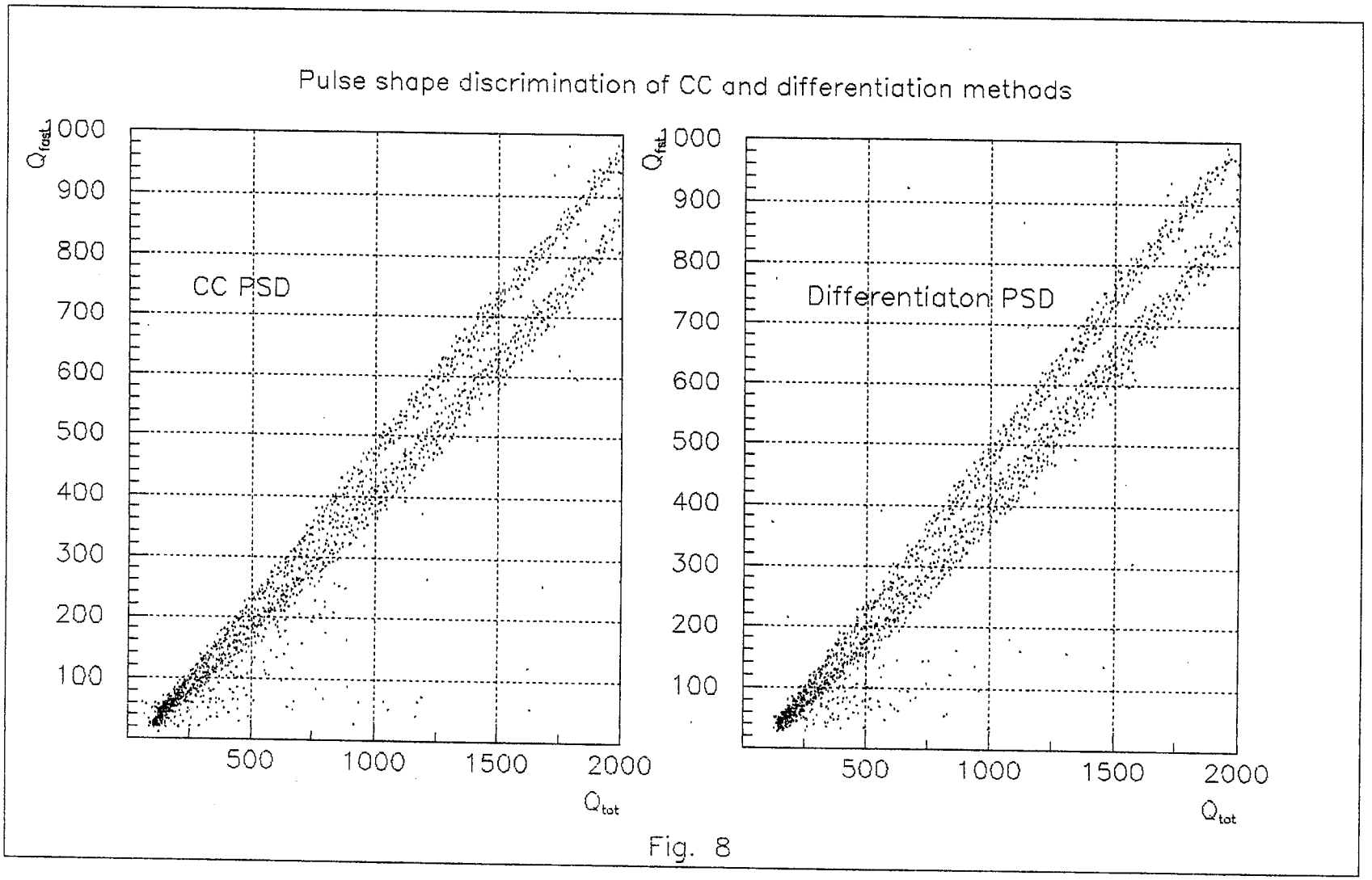
Pulse shape discrimination of CC and differentiation methods
CC PSD
Differentiaton PSD
Q_{fast}
Q_{tot}
100
200
300
400
500
600
700
800
900
1000
500
1000
1500
2000

Fig. 8

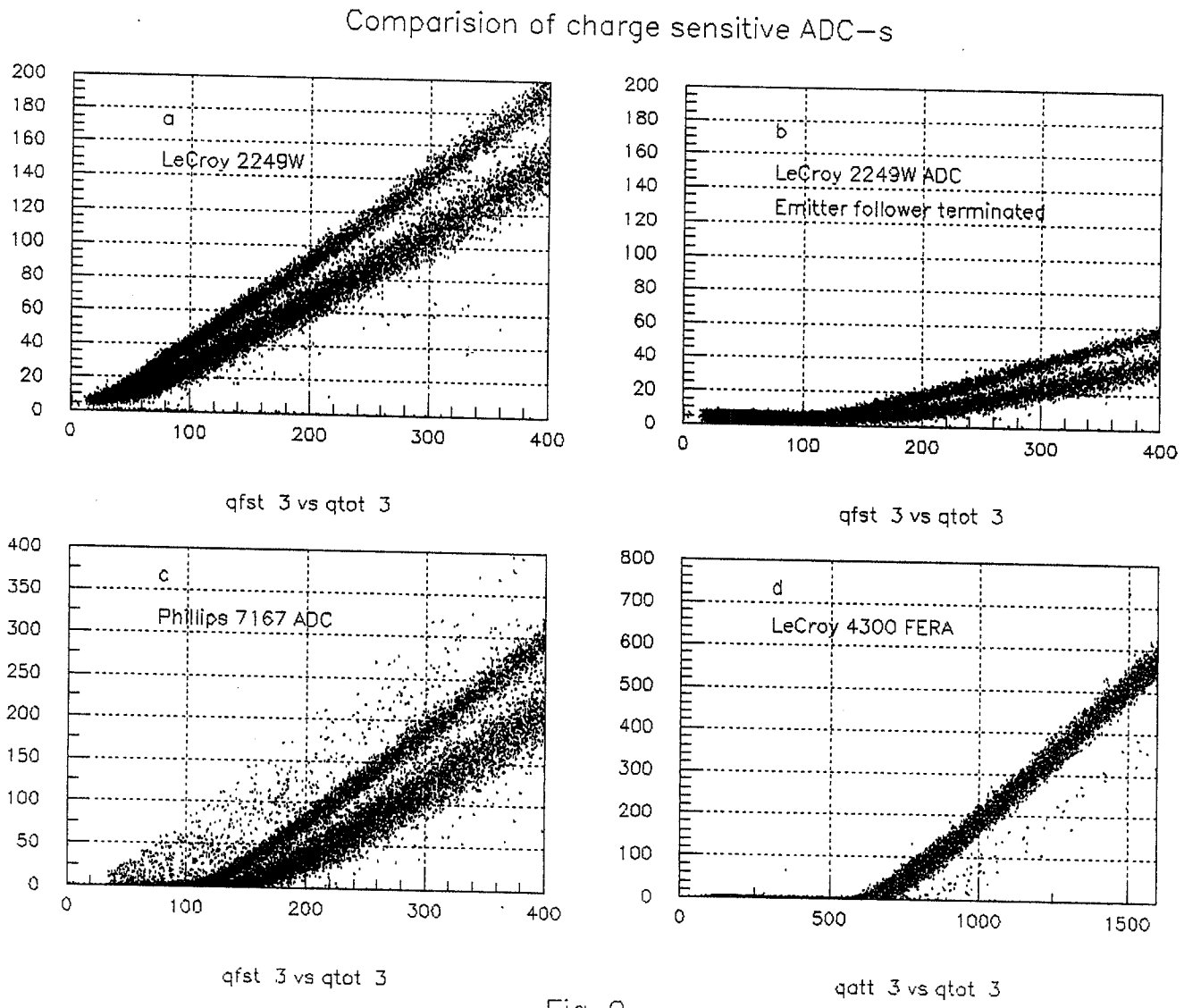
Comparision of charge sensitive ADC−s
a
LeCroy 2249W
qfst 3 vs qtot 3
b
LeCroy 2249W ADC
Emitter follower terminated
qfst 3 vs qtot 3
c
Phillips 7167 ADC
qfst 3 vs qtot 3
d
LeCroy 4300 FERA
qatt 3 vs qtot 3

Fig. 9

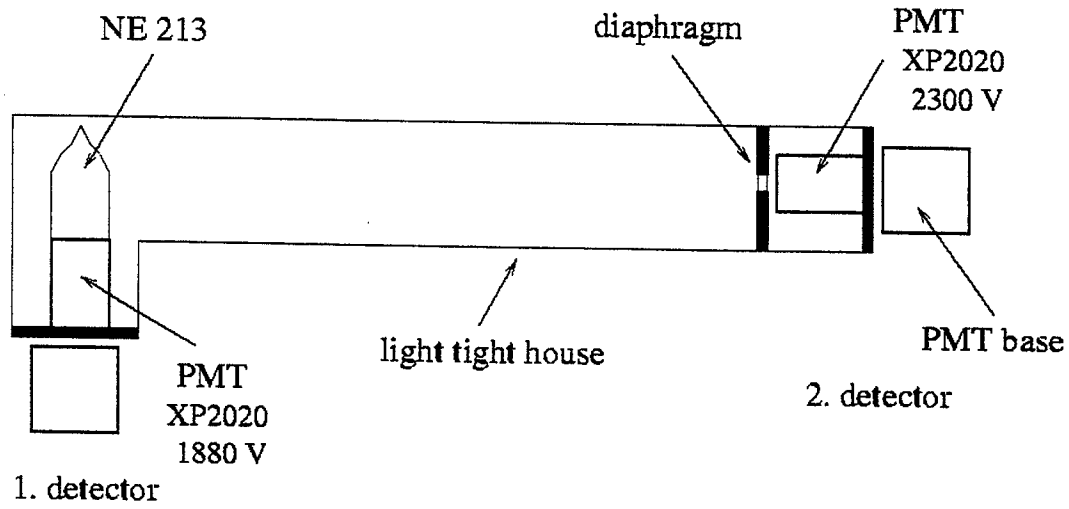
NE 213
diaphragm
PMT
XP2020
2300 V
light tight house
PMT base
2. detector
PMT
XP2020
1880 V
1. detector

Fig. 10

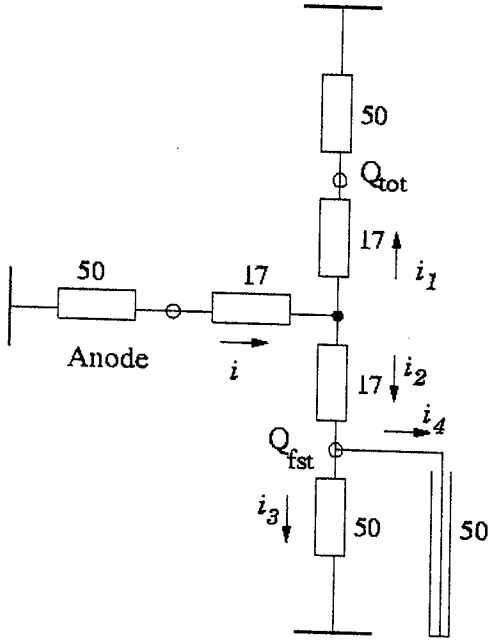

a.) 2–way splitter

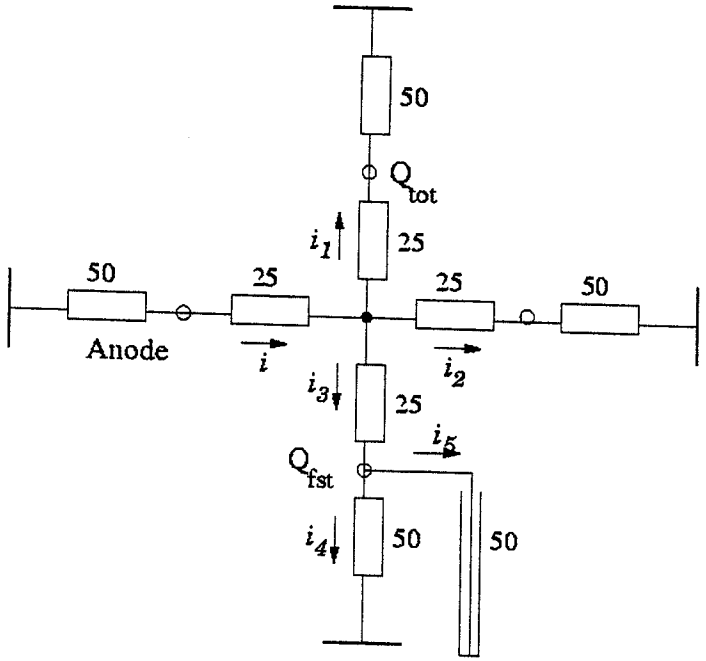

b.) 3–way splitter

$$i_{Q_{tot}} = (1 - \frac{1}{5}) \frac{42}{109} \; i$$

$$i_{Q_{fst}} = (1 - \frac{1}{2}) \frac{67}{109} \; \frac{i}{2}$$

$$i_{Q_{tot}} = (1 - \frac{1}{8}) \frac{50}{175} \; i$$

$$i_{Q_{fst}} = (1 - \frac{1}{2}) \frac{75}{175} \; \frac{i}{2}$$

Fig. 12

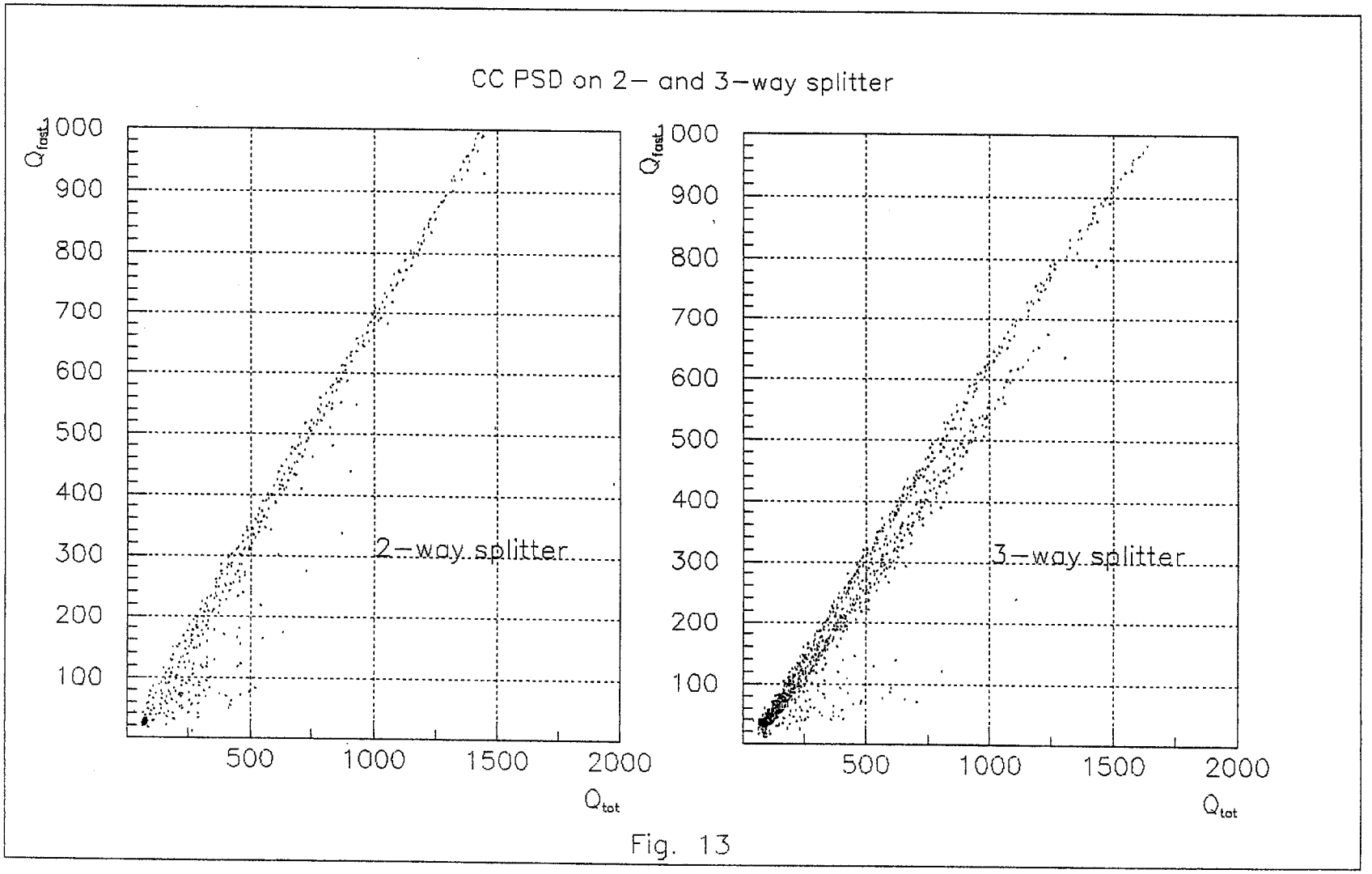
CC PSD on 2– and 3–way splitter
Q_{fast}
1000
900
800
700
600
500
400
300
200
100
2–way splitter
500
1000
1500
2000
Q_{tot}
Q_{fast}
1000
900
800
700
600
500
400
300
200
100
3–way splitter
500
1000
1500
2000
Q_{tot}

Fig. 13